JOURNAL OF GUIDANCE, CONTROL, AND DYNAMICS
Vol. 17, No. 6, November–December 1994

Analytic Time-Optimal Control Synthesis of Fourth-Order System and Maneuvers of Flexible Structures

Feiyue Li* and Peter M. Bainum†
Howard University, Washington, DC 20059

The analytic solution to the problem of minimum-time control of a fourth-order linear system near the origin is obtained by using Gulko's subsystem strategy. This system has two real eigenvalues (zeros) and two imaginary eigenvalues (vibrational frequency), which represents a flexible structure with one rigid-body mode and one flexible mode. The complete solution including the optimal switching times for the second-order subsystem is first obtained. Next, the geometry of the control switching surface near the origin for the third-order subsystem is analyzed through the phase-plane and phase-space technique. Then, the switching function for the full fourth-order system is constructed by using the roots of a quartic algebraic equation. This solution can be used to synthesize the feedback time-optimal control for the maneuvers of flexible structures. Numerical examples with one and more flexible modes are illustrated to show the applications of the solution.

Introduction

THE minimum-time or near-minimum-time large-angle slewing maneuver problem of flexible structures has gained much attention in recent years. For example, Refs. 1–6 are some of the papers related to the planar (single-axis) maneuver problems. Singh et al.[1] developed an open-loop homotopy numerical method to find the solution of the minimum-time maneuver problem with n flexible modes. Önsay and Akay[2] conducted an experiment by implementing a similar open-loop, symmetric, multiswitch bang-bang control law to a controlled model with one rigid-body mode and two flexible modes. Bainum and Li[3] presented an open-loop near-minimum-time maneuver of an unsymmetric general flexible spacecraft with n modes by using the quasilinearization and time-shortening technique. It was shown that the trade-off between the slewing time and the maximum first flexible modal amplitude during the maneuver can be made. Hablani[4] analyzed the unsymmetric effect of the structural damping on the open-loop maneuver problem with one rigid-body mode and one flexible mode. Liu and Wie[5] developed an open-loop sub-time-optimal computing algorithm based on the parameter optimization technique with robustness considerations. The resulting multiswitch control can reduce the residual vibration, and the examples with one rigid-body mode and one flexible mode were considered. Barbieri and Özgüner[6] proposed a partial closed-loop control method using feedback of the rigid-body states and the first vibrational frequency. The phase-plane technique was applied to the system with one rigid-body mode and one flexible mode.

From these investigations, we can observe the following: 1) most of the controls are open-loop strategies, 2) the first flexible mode dominates the analyses, and 3) multiswitch bang-bang control can achieve better near-minimum-time maneuvers. Clearly, there is a need to develop closed-loop control strategies. It is certainly better if the closed-loop control can handle the effects such as the uncertainty of the structural parameters, the truncation of the higher order modes, the actuator nonlinearity, etc.

The system in this paper represents a rather typical simplified structural model used for rapid large-angle rotational maneuvers of flexible spacecraft and flexible robotic arms. This model includes one rigid-body mode and one flexible mode with one collocated control input. When expressed in state-space form, the equations of motion yield fourth-order ordinary differential equations with two real eigenvalues (zeros) and two imaginary eigenvalues (vibrational frequency).

The analytic solutions for the time-optimal control of systems up to fourth order with all real eigenvalues have been obtained in the literature.[7] However, the analytic solution for third- and fourth-order systems with complex eigenvalues has not been seen in the open literature. The main obstacle to the latter problem lies in the fact that the maximum number of switches of the control is fixed for systems with real eigenvalues but is not fixed for systems with complex eigenvalues. In this paper, we will apply Gulko's strategy[7] by first analyzing the local geometry of the switching function for the third-order system (half rigid-body mode and one flexible mode) and then obtaining the local solution for the fourth-order system. This solution can be used to synthesize the feedback control for the system. More specifically, the control switching functions are expressed in terms of the state of the system, which bears important practical advantages in implementation. Applications of this solution to the maneuvers of flexible spacecraft will be illustrated by numerical examples.

Mathematical Model and Transformations

A typical fourth-order system derived from the flexible spacecraft dynamics with one rigid-body mode, one flexible mode, and one control torque input variable, without damping, can be expressed in the following matrix notation[1]:

$$\dot{q}=\bar{A}q+\bar{b}u, \qquad \bar{A}=\begin{bmatrix}0 & 1 & 0 & 0\\ 0 & 0 & 0 & 0\\ 0 & 0 & 0 & \omega\\ 0 & 0 & -\omega & 0\end{bmatrix}, \qquad \bar{b}=\begin{bmatrix}0\\ b_0\\ 0\\ b_1\end{bmatrix} \tag{1}$$

where $q=[q_1\ q_2\ q_3\ q_4]^T$ is the generalized coordinate vector, b_0 and b_1 are constants, and ω is the frequency of the flexible mode. By introducing the following nonsingular linear transformation (for the reason discussed in remark 2 of the Appendix),

$$x=Tq$$

$$T=\begin{bmatrix}1/(\omega^2 b_0) & 0 & -1/(\omega^3 b_1) & 0\\ 0 & 1/(\omega^2 b_0) & 0 & -1/(\omega^2 b_1)\\ 0 & 0 & 1/b_1 & 0\\ 0 & 0 & 0 & 1/b_1\end{bmatrix} \tag{2}$$

Received Jan. 24, 1994; revision received Feb. 25, 1994; accepted for publication Feb. 25, 1994.

*Research Associate, Department of Mechanical Engineering. Member AIAA.
†Distinguished Professor of Aerospace Engineering, Department of Mechanical Engineering. Fellow AIAA.

Eq. (1) can be transformed into the following serially decomposed system S:

$$\dot{x} = Ax + bu, \qquad A = T\bar{A}T^{-1} = \begin{bmatrix} 0 & 1 & 0 & 0 \\ 0 & 0 & 1/\omega & 0 \\ 0 & 0 & 0 & \omega \\ 0 & 0 & -\omega & 0 \end{bmatrix}$$

$$b = T\bar{b} = \begin{bmatrix} 0 \\ 0 \\ 0 \\ 1 \end{bmatrix} \tag{3}$$

To facilitate the subsequent analysis, we introduce the following two subsystems, S_{II} and S_{III}:

$$S_{II}: \qquad \dot{x}_3 = \omega x_4, \qquad \dot{x}_4 = -\omega x_3 + u_2 \tag{4}$$

$$S_{III}: \qquad \dot{x}_2 = x_3/\omega, \qquad \dot{x}_3 = \omega x_4, \qquad \dot{x}_4 = -\omega x_3 + u_3 \tag{5}$$

where u_2 and u_3 are associated controls for S_{II} and S_{III}, respectively. It is clear that subsystems S_{II} and S_{III} are imbedded in the original fourth-order system S.

Control Switching Curve of S_{II}

We now review the well-known time-optimal control solution for the subsystem S_{II}, a harmonic oscillator system. By summarizing the results obtained in the literature,[8,9] we provide the following explicit analytical expressions:

$$u_2 = -\text{sgn}[s_2(x_3, x_4)], \qquad s_2 = \begin{cases} \beta_2, & \beta_2 \neq 0 \\ -\omega x_3, & \beta_2 = 0 \end{cases} \tag{6}$$

$$\beta_2 = \omega x_4 + \text{sgn}(x_3)\sqrt{1 - (C_x - |\omega x_3|)^2} \tag{7}$$

where C_x is a function of x_3,

$$C_x = \{2n + 1, \text{ if } ||\omega x_3| - (2n + 1)| \leq 1, n = 0, 1, 2, \ldots\} \tag{8}$$

or

$$C_x = 2\left[\tfrac{1}{2}|\omega x_3|\right] + 1 \tag{9}$$

where $[x]$ is the largest integer not exceeding x.

We now discuss the main difference between this harmonic oscillator system and the double-integrator system. The switching curve (locus) for this control in the $\omega x_3 - \omega x_4$ phase plane is plotted in Fig. 1. This curve is represented by the lower semicircles centered on the ωx_3 axis at $1, 3, 5, \ldots$ and the upper semicircles centered on the ωx_3 axis at $-1, -3, -5, \ldots$. All these semicircles have a radius of 1. A typical optimal trajectory from an initial state P_0 to the origin is indicated by the curve $P_0 - P_1 - P_2 - (0, 0)$. On this trajectory, P_0P_1 is an arc centered at $(-1, 0)$ with control $u_2 = -1$. The control switches to 1 at P_1. Here P_1P_2 is an arc centered at (1, 0). The control switches again to -1 at P_2. The state then follows the arc P_20 to $(0, 0)$. It is seen that the optimal control for subsystem S_{II} can have more than one intermediate switch. This property is determined by the inherent oscillation characteristics of the flexible (vibrational) systems with complex (or imaginary) eigenvalues. The total number of switches depends on the initial state of the system. On the contrary, the optimal control for the double-integrator system

$$\dot{x}_3 = x_4, \qquad \dot{x}_4 = u_2 \tag{10}$$

has at most one intermediate switch.[7,8] Instead of circles, the switching curves for this system are represented by two segments of parabolas joined at the origin. The number of time-optimal control switches is bounded and is independent of the initial state. Moreover, this property is also true for any general normal system with real eigenvalues.[7,8]

A control synthesis strategy (see the Appendix) has been developed by Gulko et al.[7] to construct the feedback control for systems

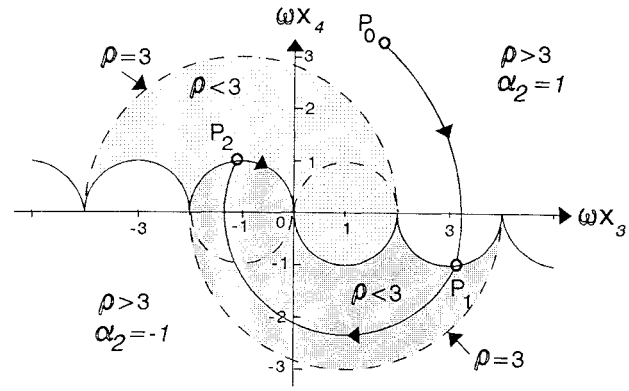

Fig. 1 Switching curve and one intermediate switching region for S_{II}.

with real eigenvalues. The proof of the optimality of this strategy depends on the condition that the number of optimal control switches is bounded. In this strategy, the original system is first decomposed into serially connected subsystems so that the lower order subsystem is decoupled from its higher order parent system. This enables the control to be first determined for the lower order system and then extended to the higher order system. It is important that each system contains the one-less-order system as its subsystem. As the order of the system increases by 1, the maximum allowable number of switches for the control also increases by 1. It is also interesting that the information needed for constructing the switching function for each system is obtained only from its immediate (adjacent) lower order system, and the results from other lower order systems are not required.

The applicability of this strategy for systems with complex (or imaginary) eigenvalues has not been demonstrated previously. As shown before, the optimal control for the system containing one or more pairs of complex-conjugate eigenvalues may require an arbitrary number of intermediate switches. This increases the difficulty in obtaining the solution for higher order systems by using the information from the corresponding lower order systems. However, in this paper, we would like to use this strategy to obtain some conditional solutions under some constraints, for example, assuming that the maximum number of switches is fixed. This solution is then referred to as the local solution. The validation of this solution in a certain region of the state space will be checked by using numerical methods.

Optimal Switching Times for S_{II}

We now need to find the switching times for S_{II} in order to construct the switching functions for S_{III}. In the beginning, we consider the case with one intermediate switch. Let t_1 represent this switching time and t_2 represent the terminal time. By integrating Eq. (4) and using the initial state vector $[x_3 \quad x_4]^T$ we can obtain

$$\begin{cases} 2\sin\theta_1 - \sin\theta_2 = \text{sgn}(s_2)\omega x_4 \\ 2\cos\theta_1 - \cos\theta_2 = 1 + \text{sgn}(s_2)\omega x_3 \end{cases} \tag{11}$$

where $\theta_1 = \omega t_1$, and $\theta_2 = \omega t_2$. By performing algebraic and trigonometric operations on Eq. (11), such as squaring both sides of the equation, we can obtain

$$\theta_1 = \varphi + \varphi_1, \qquad \theta_2 = \varphi + \varphi_2 \tag{12}$$

where

$$\varphi = \tan^{-1}\frac{\alpha_2\omega x_4}{1 + \alpha_2\omega x_3}, \qquad \alpha_2 = \text{sgn}(s_2) \tag{13}$$

$$\varphi_1 = \cos^{-1}\frac{3 + \rho^2}{4\rho}, \qquad \varphi_2 = \cos^{-1}\frac{3 - \rho^2}{2\rho}$$

$$1 \leq \rho \leq 3 \tag{14}$$

and

$$\rho^2 = \rho_x^2 + \rho_y^2 = (1 + \alpha_2\omega x_3)^2 + (\omega x_4)^2 \tag{15}$$

To guarantee the validity of Eq. (14), ωx_3 and ωx_4 should be within the shaded region plotted in Fig. 1. Within this region, the range of φ is $[-\frac{1}{6}\pi, \pi]$. It can be proven that another candidate solution also satisfies Eq. (11),

$$\theta_1 = \varphi - \varphi_1, \qquad \theta_2 = \varphi + 2\pi - \varphi_2 \tag{16}$$

It is clear that the θ_2 in Eq. (16) is larger than the θ_2 in Eq. (12). Therefore, Eq. (12) is the minimum-time solution for the subsystem S_{II}.

For the general case with multiple intermediate switches, we have obtained the following solutions for the switching times:

$$\delta = 2\left[\tfrac{1}{2}(\rho + 1)\right] \tag{17}$$

where $n = \frac{1}{2}\delta$ is the number of intermediate switches;

$$\theta_i = \omega t_i \tag{18}$$

where t_{n+1} is the total time;

$$\varphi_1 = \cos^{-1}\frac{\rho^2 + \delta^2 - 1}{2\delta\rho}, \qquad \varphi_{n+1} = \cos^{-1}\frac{(-1)^n(\rho^2 - \delta^2 + 1)}{2\rho} \tag{19}$$

and

$$\begin{cases} \theta_1 = \varphi + \varphi_1, & \theta_2 = \pi + \theta_1, \\ \theta_n = \pi + \theta_{n-1}, & \theta_{n+1} = \varphi + \left[\frac{1}{2}n\right]2\pi - (-1)^n\varphi_{n+1} \end{cases} \tag{20}$$

where φ and ρ defined in Eqs. (13) and (15) and $[x]$ is the largest integer not exceeding x.

Local Control Switching Geometry of S_{III}

From the system S_{III} in Eq. (5), we have

$$A_3 = \begin{bmatrix} 0 & 1/\omega & 0 \\ 0 & 0 & \omega \\ 0 & -\omega & 0 \end{bmatrix} \qquad b_3 = \begin{bmatrix} 0 \\ 0 \\ 1 \end{bmatrix}$$

$$e^{A_3 t} = \begin{bmatrix} 1 & \sin\omega t/\omega^2 & (1 - \cos\omega t)/\omega^2 \\ 0 & \cos\omega t & \sin\omega t \\ 0 & -\sin\omega t & \cos\omega t \end{bmatrix} \tag{21}$$

By assuming one intermediate switch for subsystem S_{II} and using Eq. (11), we can obtain the integral

$$\int_0^{t_1} e^{-A_3 t} b_3\, dt - \int_{t_1}^{t_2} e^{-A_3 t} b_3\, dt = \begin{bmatrix} \frac{1}{\omega^3}(2\theta_1 - \theta_2) - \frac{1}{\omega^2}x_4\,\mathrm{sgn}(s_2) \\ x_3\,\mathrm{sgn}(s_2) \\ x_4\,\mathrm{sgn}(s_2) \end{bmatrix} \tag{22}$$

The expression in Eq. (A7) of the Appendix for the present case can be written as

$$\begin{bmatrix} \beta(x) \\ 0 \\ 0 \end{bmatrix} = e^{A_3 t_2}\left[x - \mathrm{sgn}(s_2)\left(\int_0^{t_1} e^{-A_3 t} b_3\, dt - \int_{t_1}^{t_2} e^{-A_3 t} b_3\, dt\right)\right] \tag{23}$$

The first element of this vector is the switching function for the system, S_{III},

$$\beta(x) = \beta_3' = x_2 + x_4/\omega^2 - \alpha_2(2\theta_1 - \theta_2)/\omega^3 \tag{24}$$

The problem now is whether the values of θ_1 and θ_2 from Eq. (12) or from Eq. (16) should be used. Intuitively, we should first pick Eq. (12) since it is the minimum-time solution for S_{II}. However, for some initial conditions of $[x_2, x_3, x_4]^T$, this choice does not result in a valid solution for the third-order system. We will discuss this point by using an example. By introducing the new variable

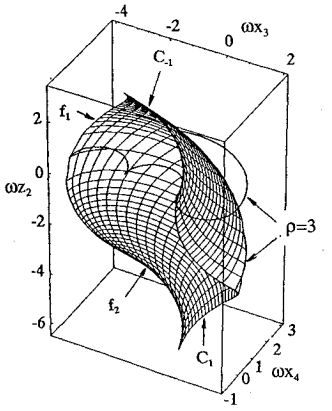

Fig. 2 Part of switching surface for S_{III} ($\alpha_2 = 1$).

$$z_2 = \omega^2 x_2 + x_4 \tag{25}$$

Eqs. (5) and (24) (multiplied by ω^3) can be expressed as

$$\dot{z}_2 = u, \qquad \dot{x}_3 = \omega x_4, \qquad \dot{x}_4 = -\omega x_3 + u \tag{26}$$

$$\beta_3 = \omega z_2 - \alpha_2(2\theta_1 - \theta_2) \tag{27}$$

Now we define two functions f_1 and f_2 in the three-dimensional space (z_2, x_3, x_4) by substituting Eqs. (12) and (16) into Eq. (27):

$$f_1\colon\ \omega z_2 - \alpha_2(\varphi + 2\varphi_1 - \varphi_2) = 0 \tag{28}$$

$$f_2\colon\ \omega z_2 - \alpha_2(\varphi - 2\varphi_1 + \varphi_2 - 2\pi) = 0 \tag{29}$$

These functions represent two different switching surfaces in the valid region determined by Eq. (14). A part of the surfaces ($\alpha_2 = 1$) is shown in Fig. 2. The function f_2 is lower than f_1 according to the z_2 coordinate. They join together by a space curve at $\rho = 3$, (shown both in space and in the ωx_3-ωx_4 plane in Fig. 2) determined by

$$f_1 \equiv f_2 : \varphi + 2\varphi_1 - \varphi_2 = \varphi - 2\varphi_1 + \varphi_2 - 2\pi \tag{30}$$

Also shown in Fig. 2 are C_1 and C_{-1}, the helical curves in space about (1, 0) and (−1, 0), respectively. The surface f_1 contains the helical curve formed by z_2 and the lower half unit circle about (1,0), $\omega x_4 = -[1 - (\omega x_3 - 1)^2]^{1/2}$, and f_2 contains a helical curve formed by z_2 and the upper half unit circle about (1,0), $\omega x_4 = [1 - (\omega x_3 - 1)^2]^{1/2}$.

We now examine an arbitrary point $(\omega z_2, \omega x_3, \omega x_4) = (-4.1838, 0.1, 1.9)$ on f_2. Before the trajectory reaches this point, it is moving upward (increasing z_2), because the trajectory is below both f_1 and f_2 and, therefore, $u_2 = 1$ and $u_3 = 1$. For this point, $u_2 = 1$ from Eq. (6). If we use f_1 as the switching surface, we have $f_1 = -4.1764$. According to Eq. (28), $u_3 = -\mathrm{sgn}(f_1) = 1$. This means that the trajectory of the system S_{III} will continue to move along a circle about (1, 0) and eventually go out of the valid region, bounded by $\rho = 3$. Once the trajectory moves out of the region, it will require more switches to bring the trajectory back to the origin than when it is inside the region. As a result of this, more switches imply longer time to be used for the trajectory to reach the origin. Therefore, it is certainly not the time-optimal solution. On the other hand, if we use f_2 as the switching function, the control will switch right on this point, i.e., $u_3 = -\mathrm{sgn}(-f_2) = -1$. This control will confine the trajectory within the boundary, $\rho = 3$. The projected trajectory onto the ωx_3-ωx_4 phase plane will intersect the upper half unit circle about (1, 0), and the control will switch to $u_3 = 1$ until the trajectory reaches the origin. This trajectory is clearly the optimal trajectory for this example, although the motion of its second-order subsystem is not optimal. This result is quite different from that of the system with real eigenvalues.[7] For those systems, the optimal solution for the subsystem must be used. This is the essential difference between the systems with real eigenvalues and the systems with complex eigenvalues.

The reason for this can be made clear if we compare our current system with the system that contains the double-integrator system. In the double-integrator subsystem, the switching curves are formed by joining two halves of two parabolas at the origin. The other two halves are thrown away because they tend to lead the trajectory to infinity. This switching curve is a monotone curve stretched over the whole phase plane. In three dimensions, this curve is contained in the optimal switching surface extending to infinity. Once the trajectory hits this surface, it will stay on this surface, approach the curve, and move to the origin.

For our current system, the two-dimensional switching curve of the subsystem is composed of semicircles as in Fig. 1. We also throw the other half away. But unlike the parabolic case, the trajectory on the abandoned half circle is limited in magnitude, i.e., it will not go to infinity. These abandoned curves are also candidate switching curves, although they are not optimal switching curves. But this does exclude the possibility that, in three-dimensional space, these abandoned curves may become part of the optimal switching surface. This argument has just been validated by the previous example, where the control switched at this abandoned upper half circle and the trajectory follows this curve and the lower half circle to the origin. Since the "head" of the circle will meet its "tail" in the phase plane, we can imagine that the optimal switching surface in the three-dimensional space will be tortured, unlike the pretty "straight" appearance of the parabolic surface. For the current system with imaginary eigenvalues, the trajectory of the system will generally hit the candidate switching surfaces many times. The important point is to find the criterion identifying when to use which surface as the switching surface. To find this rule, we need to consider the relation between the trajectory and these candidate surfaces.

Middle Layer Between f_1 and f_2

We now assume that there is a middle layer in the space between the two surfaces f_1 and f_2 such that the trajectory above this layer will reach f_1 and the trajectory below it will reach f_2. Therefore, the trajectory on this layer will hit the boundary curve, $\rho = 3$ as mentioned above, between the two surfaces. This layer will provide a rule that determines which candidate surface should be used as the switching function for the third-order system.

Since this layer is determined by the trajectory of the third-order system, an initial point $P_0(z_{20}, x_{30}, x_{40})$ on this layer should satisfy Eq. (26). Here the control u takes the value before the trajectory hits the switching surfaces. By integrating Eq. (26) and eliminating the time t, we have the following relations between two points P_0 and $P(z_2, x_3, x_4)$ on the same trajectory:

$$(\omega x_3 - \alpha)^2 + (\omega x_4)^2 = (\omega x_{30} - \alpha)^2 + (\omega x_{40})^2 = \rho_0^2 \tag{31}$$

$$\omega(z_2 - z_{20}) = \alpha(\varphi_0 - \bar{\varphi}), \qquad \varphi_0 = \cos^{-1}\frac{\omega x_{30} - \alpha}{\rho_0}$$
$$\bar{\varphi} = \cos^{-1}\frac{\omega x_3 - \alpha}{\rho_0} \tag{32}$$

where α takes the same value of the control before the trajectory hits the switching surface. If (x_{30}, x_{40}) and (x_3, x_4) are known, the difference in the z_2 coordinate between P_0 and P can be obtained from Eq. (32).

When point P hits the boundary curve, $\rho = 3$, it should satisfy

$$\omega z_2 = \alpha(2\theta_1 - \theta_2), \qquad (\omega x_3 + \alpha)^2 + (\omega x_4)^2 = \rho^2 = 3^2 \tag{33}$$

where θ_1 and θ_2 are defined in either Eq. (12) or Eq. (16). By substituting $\rho = 3$ into Eqs. (13) and (14) and replacing the function arctangent by arccosine in Eq. (13) by considering the fact that, for $\rho = 3$, the range of φ is $[0, \pi]$ and the principal value of arccosine is also $[0, \pi]$, we have

$$\varphi_1 = 0, \qquad \varphi_2 = \pi,$$
$$\tilde{\varphi} = \varphi = \cos^{-1}\frac{1 + \alpha\omega x_3}{\rho} = \cos^{-1}\frac{1 + \alpha\omega x_3}{3} \tag{34}$$

The second equation in Eq. (33) can be rewritten as

$$(\omega x_3 + \alpha)^2 + (\omega x_4)^2 = (\omega x_3 - \alpha)^2 + (\omega x_4)^2 + 4\alpha\omega x_3 = 9 \tag{35}$$

Substituting Eq. (31) into Eq. (35), we obtain

$$\rho_0^2 + 4\alpha\omega x_3 = 9 \qquad \text{or} \qquad \omega x_3 = \frac{1}{4}\alpha(9 - \rho_0^2) \tag{36}$$

Using this result, $\bar{\varphi}$ in Eq. (32) and $\tilde{\varphi}$ in Eq. (34) can be rewritten as

$$\bar{\varphi} = \cos^{-1}\frac{\alpha(5 - \rho_0^2)}{4\rho_0}, \qquad \tilde{\varphi} = \cos^{-1}\frac{13 - \rho_0^2}{12} \tag{37}$$

Combining the first equations of Eqs. (32) and (33), we have the expression for the middle separation layer f_{12}:

$$f_{12}: \quad \omega z_{20} - \alpha(\bar{\varphi} - \pi - \varphi_0 + \tilde{\varphi}) = 0 \tag{38}$$

Intersection of Trajectory and f_2

Since the space between f_1 and f_2 (Fig. 2) can be divided into two regions by the middle separation layer f_{12}, the points in the upper region will hit f_1, and the points in the lower region will reach f_2. Then, what will happen for the trajectory points below f_2? Are they not going to reach f_2 at all? If they are, they will enter the lower region and then, according to the previous discussion, tend to move out of this region by hitting f_2 again. In other words, they will hit f_2 twice. Let us assume the situation exists and try to find them. According to the uniqueness theory of the solutions of the linear ordinary differential equations, the trajectories for different initial conditions for the present system will not run into each other in this region (there are no conjugate points); i.e., they are "parallel" in space and form a field. Therefore, there must exist some limiting points, whose trajectories will hit f_2 only once; i.e., they are tangent to f_2. Then, all these tangent points on f_2 form a space curve. If we can identify this curve, we will have the knowledge of how to use f_2 as the optimal switching function.

That the trajectory is tangent to f_2 implies that the tangent line of the trajectory is perpendicular to the normal line of the surface f_2. From Eq. (26), we can obtain the direction cosine of the tangent line of the trajectory of the third-order system:

$$\frac{l}{\alpha} = \frac{m}{\omega x_4} = \frac{n}{\alpha - \omega x_3} \tag{39}$$

where α takes the value of u before the trajectory reaches the surface, f_2. On the other hand, the direction cosine of the normal line for f_2 in Eq. (29) can be written as

$$\frac{L}{f'_{z_2}} = \frac{M}{f'_{x_3}} = \frac{N}{f'_{x_4}} \tag{40}$$

and

$$f'_{z_2} = -\omega, \qquad f'_{x_3} = \alpha\frac{\partial}{\partial x_3}(2\theta_1 - \theta_2)$$
$$f'_{x_4} = \alpha\frac{\partial}{\partial x_4}(2\theta_1 - \theta_2) \tag{41}$$

where the subscript 2 for f_2 has been omitted. The condition for these two lines to be perpendicular can be expressed by

$$0 = lL + mM + nN = \alpha f'_{z_2} + \omega x_4 f'_{x_3} + (\alpha - \omega x_3) f'_{x_4} \tag{42}$$

By using Eq. (29) for f_2 and carrying out all the partial derivatives in Eq. (41), we can obtain

$$\alpha\rho^2 = \alpha(1 + \alpha\omega x_3) + 3\omega x_4\sqrt{\rho^2 - 1}\Big/\sqrt{9 - \rho^2} \tag{43}$$

After further simplification, we can obtain one equation for the required curve,

$$(\alpha\omega x_3 + 2)^2 + (\omega x_4)^2 = \rho_2^2 = 4 \tag{44}$$

This is the projection of the tangent curve onto the ωx_3-ωx_4 phase plane. It is a circle of radius 2 centered at $(-2, 0)$ or $(2, 0)$ of the phase plane, as shown in Fig. 3.

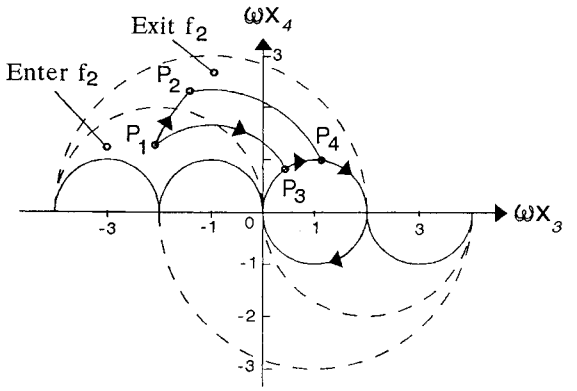

Fig. 3 f_2 entry and exit regions.

Optimal Switching Point on f_2

As shown in Fig. 3, a general trajectory that enters the lower region at point P_1 on f_2 will exit at point P_2 on f_2. Therefore, there are two possible paths, P_1-P_3-P_4-(0, 0) and P_1-P_2-P_4-(0, 0), that the trajectory can follow to reach the origin. We may wonder which path takes less time and, thus, can be used as the optimal trajectory. We now examine this. If we replace the coordinates ωx_3 and ωx_4 by the following parameters, R and γ,

$$1 - \alpha\omega x_3 = R\cos\gamma, \qquad \omega x_4 = R\sin\gamma \tag{45}$$

the time required for a trajectory of the system to travel from $P_1(\omega x_3, \omega x_4)$ on f_2 through P_3 to (0, 0) can be considered as the function of R and γ, and it is proportional to $\theta_2 = \omega t_2$,

$$\theta_2(R, \gamma) = \varphi(R, \gamma) + 2\pi - \varphi_2(R, \gamma) \tag{46}$$

Similarly, the time required from point $P_2[\omega(x_3 + \Delta x_3), \omega(x_4 + \Delta x_4)] = P_2(R, \gamma + \Delta\gamma)$ to (0, 0) is

$$\theta_2(R, \gamma + \Delta\gamma) = \varphi(R, \gamma + \Delta\gamma) + 2\pi - \varphi_2(R, \gamma + \Delta\gamma) \tag{47}$$

where Δ is the incremental symbol. Since the motion from P_1 to P_2 is on the circle of radius R with center at (1, 0) of the phase plane, R is not changed. The time used from P_1 to P_2 is $\Delta t = \Delta\gamma/\omega$. Then, the time difference between these two paths is proportional to

$$\Delta\theta_2 = \Delta\gamma + \varphi(\gamma + \Delta\gamma) - \varphi(\gamma) - [\varphi_2(\gamma + \Delta\gamma) - \varphi_2(\gamma)] \tag{48}$$

When $\Delta\gamma \to 0$, we have the following derivatives of the traveling time (multiplied by ω):

$$\frac{d\theta_2}{d\gamma} = 1 + \frac{d\varphi}{d\gamma} - \frac{d\varphi_2}{d\gamma} \tag{49}$$

By performing all required differentiations and simplifications, we can obtain

$$\frac{d\theta_2}{d\gamma} = \frac{2}{\rho^2}\left[(1 + \alpha\omega x_3) - \frac{\alpha(3 + \rho^2)\omega x_4}{\sqrt{4\rho^2 - (3 - \rho^2)^2}}\right] \tag{50}$$

It is easy to verify that, for the region in the phase plane considered here, the derivative is always less than zero. This means that the second path, P_1-P_2-P_4-(0, 0), takes less time and that the exit point on f_2, not the entry point, is the optimal switching point.

Switching Function for $\rho > 3$

All the previous discussions are based on the assumption $\rho \le 3$. We now consider the case in which $\rho > 3$ and the second-order subsystem has two intermediate switches. We assume that the third-order system also requires two intermediate switches. By integrating Eq. (5) and using Eq. (A7), we can obtain the following switching surface:

$$\beta_3'' = x_2 + \frac{x_4}{\omega^2} - \frac{\alpha_2}{\omega^5}[2(\theta_1 - \theta_2) + \theta_3] \tag{51}$$

From this result we can see that the switching surface depends on only θ_3 and the difference between θ_1 and θ_2. If we use the optimal solution for the second-order subsystem from the general solution Eq. (20) by setting $n = 2$, we can have $\theta_2 = \pi + \theta_1$ and the switching surface

$$f_3\colon \omega z_2 - \alpha_2(\theta_3 - 2\pi) = 0 \tag{52}$$

$$\theta_3 = \varphi + 2\pi - \varphi_3, \qquad \varphi_3 = \cos^{-1}\frac{\rho^2 - 15}{2\rho} \tag{53}$$

The validation of this switching function has been proven by using several numerical examples in the neighborhood of the origin. The testing procedure can be described as follows. The reference numerical results (correct optimal solution) are first obtained by using a different numerical method, called the shooting method. Then the numerical results from the analytical solution are compared to the reference results.

By summarizing all the above results, we can have the following control switching policy for system S_{III}:

$$u_3 = -\text{sgn}[s_3(x_2, x_3, x_4)], \qquad s_3 = \begin{cases} \beta_3, & \beta_3 \neq 0 \\ s_2, & \beta_3 = 0 \end{cases} \tag{54}$$

$$\beta_3 = \left\{\begin{array}{ll} -f_2 & \text{if } \rho > 1, \rho_2 > 2, f_{12} < 0 \\ f_1 & \text{otherwise} \\ f_3 & \text{if } \rho > 3 \end{array}\right\} \quad \text{if } \rho \le 3 \tag{55}$$

where the definitions of ρ, f_1, f_2, f_{12}, ρ_2, and f_3 can be found from Eqs. (15), (28), (29), (38), (44), and (52), respectively. In most of our numerical tests, the condition $\rho \le 3$ is satisfied; i.e., one intermediate switch for the second-order subsystem is required.

Control of Fourth-Order System S

By using Eq. (A7), the switching function for the fourth-order Eq. (3) can be obtained:

$$\beta_4(x) = \omega^4 x_1 + \omega x_3 + \alpha_3\left(\theta_1^2 - \theta_2^2 + \tfrac{1}{2}\theta_3^2\right) \tag{56}$$

where $\alpha_3 = \text{sgn}(s_3)$, $\theta_i = \omega t_i$. Note that, in this method, the hardest task is not getting the above formula, but finding the analytical solution to the optimal switching times t_i of the third-order subsystem. Once the t_i are determined, the control for the system is determined by

$$u = u_4 = -\text{sgn}(s_4), \qquad s_4 = \begin{cases} \beta_4, & \beta_4 \neq 0 \\ s_3, & \beta_4 = 0 \end{cases} \tag{57}$$

The Solution of θ_i

By assuming three switches for S_{III} and integrating Eq. (5), we have

$$\begin{aligned} 2\theta_1 - 2\theta_2 + \theta_3 &= \alpha_3(\omega^3 x_2 + \omega x_4) = \gamma \\ 2(\cos\theta_1 - \cos\theta_2) + \cos\theta_3 &= 1 + \alpha_3 x_3 \\ 2(\sin\theta_1 - \sin\theta_2) + \sin\theta_3 &= \alpha_3 x_4 \end{aligned} \tag{58}$$

where $\theta_i = \omega t_i$. From the last two equations of Eq. (58), we can have

$$8\cos(\theta_2 - \theta_1) - 2\rho\cos(\theta_3 - \varphi) = 7 - \rho^2 \tag{59}$$

where φ and ρ have the same definitions as in Eqs. (13) and (15), except that α_2 is replaced by α_3. If we substitute the first equation of Eq. (58) into this equation, we can obtain

$$8\cos\left[\tfrac{1}{2}(\theta_3 - \gamma)\right] - 2\rho\cos(\theta_3 - \varphi) = 7 - \rho^2 \tag{60}$$

The solution of this equation for θ_3 will result in a quartic equation. The finding of the roots of the algebraic quartic equation has some standard procedures.[10] We now outline the key steps in finding the solution. Let

$$\begin{aligned} \theta &= \tfrac{1}{2}(\theta_3 - \gamma), & \xi &= \varphi - \gamma \\ \theta_3 - \varphi &= 2\theta - \xi, & v &= \cos\theta \end{aligned} \tag{61}$$

Table 1 Comparison of some numerical examples

	Example 1		Example 2		Example 3		Example 4	
Parameter	Ref. 1	Ours	Ref. 5	Ours	Ref. 6	Ours	Ref. 6	Ours
SW time, s								
t_1	4.2133	4.22	1.003	1.01	—	0.81	—	0.87
t_2	4.7251	4.73	2.109	2.11	—	2.15	—	1.03
t_3	5.2368	5.24	3.215	3.22	—	3.48	—	1.19
t_4	9.4501	9.45	4.218	4.22	4.2819	4.28	2.0499	2.05
Norm[a] at t_4	—[b]	0.046	—	0.0022	—	0.0069	—	0.0001
ω, rad/s	1.1507		1.414		1.0		5.0	
x_1	16.457		1.0		1.0		0.04	
b_0	0.072047		0.5		1.0		1.0	
b_1	7.080996		0.5		1.0		1.0	

[a]Norm refers to the norm of the state, x, in Eq. (3).
[b]Indicates data not available.

and by using trigonometric and algebraic operations on Eq. (60), we obtain a quartic equation for v,

$$4b^2v^4 - 8acv^3 + 4(a^2 - b^2 + c)v^2 - 4adv + d^2 = 0 \qquad (62)$$

where

$$a = \frac{4}{7-\rho^2}, \qquad b = \frac{2\rho}{7-\rho^2}$$
$$c = b\cos\xi, \qquad d = 1 - c \qquad (63)$$

To obtain the solution of this equation, we need to solve an auxiliary cubic equation for w,

$$w^3 + q_3 w + r_3 = 0 \qquad (64)$$

whose coefficients can be obtained as

$$q_3 = -\tfrac{1}{3}A^2 + dB, \qquad r_3 = -\tfrac{2}{27}A^3 + \tfrac{1}{3}dA\,B + d^2D \qquad (65)$$

$$A = a^2 - b^2 + c, \qquad B = 2a^2c - b^2d$$
$$D = b^2(c - b^2) - a^2c^2 \qquad (66)$$

One of the solutions of Eq. (64) has the standard forms

$$w = \left(-\tfrac{1}{2}r_3 + \sqrt{Q}\right)^{1/2} + \left(\tfrac{1}{2}r_3 - \sqrt{Q}\right)^{1/2}$$
$$\text{if} \qquad Q = \tfrac{1}{4}r_3^2 + \tfrac{1}{27}q_3^3 \geq 0 \qquad (67)$$

and if $Q < 0$,

$$w = 2R^{1/3}\cos\left(\tfrac{1}{3}\Omega\right), \qquad R = \sqrt{-\tfrac{1}{27}q_3^3}$$
$$\Omega = \tan^{-1}\left(-2\sqrt{-Q}/r_3\right) \qquad (68)$$

The four roots of v of Eq. (62) have the forms

$$v_{1,2} = -\tfrac{1}{2}(p-g) \pm \sqrt{P_1}, \qquad v_{3,4} = -\tfrac{1}{2}(p+g) \pm \sqrt{P_2} \qquad (69)$$

where

$$p = -\frac{ac}{b^2}, \qquad q = \frac{A}{b^2}$$
$$r = -\frac{ad}{2b^2}, \qquad s = \frac{d^2}{4b^2} \qquad (70)$$

and g, h satisfy

$$g^2 = 2k + p^2 - q \qquad \text{or} \qquad h^2 = k^2 - s$$
$$gh = kp - r \qquad\qquad gh = kp - r \qquad (71)$$

$$k = (w + A/3)/2b^2 \qquad (72)$$

In our numerical tests, roots v_3 and v_4 are sometimes complex numbers and therefore are not considered for the final solutions. As in Ref. 7, v_2 is smaller than v_1. Therefore, v_2 is used to obtain the largest θ in Eq. (61), which is the choice for the system with real eigenvalues in Ref. 7. In our current system, we need to choose v_1 when the condition $\theta_3 - \theta_2 > \pi$ is satisfied. This choice is the result of the conclusion that the path in Fig. 3. [P_1-P_2-P_4-(0, 0)] is the time-optimal trajectory.

Numerical Examples

Due to the difficulty in obtaining the explicit expression for the solution developed in the paper, we have established a numerical program to test the validity of the solution in the neighborhood of the origin of the state space. In this program, the fourth-order differential Eq. (3) is solved by using the Runge-Kutta-Merson variable-step-size integration method. A brief description of the program follows. When the state of the system, x, is available at time t, the sign of u_2 is determined by Eq. (6). Then, Eqs. (54) and (55) are used to find u_3. Next, by solving Eq. (58) for θ_i numerically, we obtain β_4 in Eq. (56) and final u in Eq. (57). Since these computations are based only on the state and no a priori knowledge of the number of switches is required, the control is in feedback form. However, the solution is valid only in the neighborhood of the origin because its derivation is based on the knowledge of a limited number of switches. The extension of this solution to the global space needs further investigation.

We have tested many numerical examples including the time-optimal example in Ref. 5, some examples in Ref. 6, and the one-mode example in Ref. 1. Table 1 lists some of the results and associated parameters. The results show that our results are the same as those of the references within given numerical accuracy. The basic integration step size $t = 0.01$ s. The integration time (simulation time) is several seconds longer than the minimum time. The norms of the state of Eq. (3) are also listed for reference. Note that all examples in the references are rest-to-rest maneuvers. But the solution in this paper can also allow us to perform the "motion-to-rest" maneuvers. The minimum time for the maneuver by our method is not known until the maneuver is finished.

The 90-deg time-optimal rest-to-rest maneuver of the structural model of Ref. 1 with 10 flexible modes ($\omega_i = 1.1507, 3.009, 7.529, 14.546, 23.962, 35.752, 49.91, 66.43, 85.31, 106.58$ rad/s) (22nd-order linear system equations) is also computed and the results are shown in Fig. 4. Each mode is represented by two equations similar to the last two of Eq. (1), where the associated control influence coefficients for the modes are $b_i = 7.081, -1.758, 0.2843, -0.0794, 0.0308, -0.0146, 0.0081, -0.0048, 0.003, -0.002$. In the simulation, only the rigid and the first flexible mode are under control; i.e., only the rigid-body motion and the first flexible mode are fed back. The first four equations [i.e., Eq. (1)] are transformed to Eq. (3) for the construction of the control signal. The tip displacement of the flexible beam in the model is given by

$$y_{\text{tip}} = \sum_{i=1}^{10} c_i q_{2i+1}$$

where q_i are states of the 22nd-order system and c_i are the associated coefficients: $c_i = -3.052, 0.443, -1.675, -0.785, -1.305, -0.961, -1.243, -1.042, -1.197, -1.064$. y_{tip} is plotted in Fig. 4b, which is similar to the response of the first modal am-

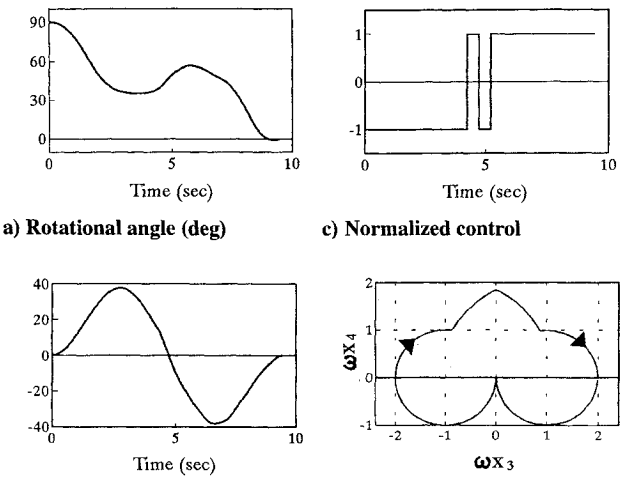

a) Rotational angle (deg) c) Normalized control

b) Tip displacement (m) d) First modal phase-plane

Fig. 4 90-deg rest-to-rest maneuver using 10 flexible modes.

plitude. Therefore, the first mode dominates the tip displacement of the beam. These results demonstrate the validity and applicability of the current solution. As far as the implementation is concerned, the computational time for each integration step (decision-making step) is usually machine dependent. The solution of the 22nd-order system differential equations by using the Runge-Kutta fixed-step-size integration method, from $t = 0$ to $t = 9.6$ s, with integration step size $t = 0.01$ s (total 960 steps), requires 0.78 s central processing unit (CPU) time [including input/output (I/O)] on an IBM/9121/44 mainframe. This means that each step requires 0.00081 s. For a mission with a sampling time $t = 0.01$ s and a computer of slower speed, the delay due to the calculation at each step should be very small. We believe that a refined program can further reduce the computational time.

In this application, the small effect of higher order modes on the control based on the first mode may be due to the separation in the frequencies of the flexible modes of the system. The application to other types of flexible systems with more densely packed modes needs to be investigated. In that case, the coupling, for example, between modes 1 and 2, may be very strong and the second mode may have to be included in the control design model.

Conclusion

In this paper, the complete solution of the time-optimal control problem of the second-order system has been obtained. The local solutions for the time-optimal controls of the third- and fourth-order systems have been obtained by applying Gulko's subsystem approach. In applying this approach, the nonoptimal solution for the subsystem must also be used in constructing the switching functions of the higher order system, which is not true for systems with real eigenvalues. Due to the periodic characteristics of the switching curves of the second-order subsystem with imaginary eigenvalues, the switching surface of the third-order system displays a quite complicated and interesting shape. By using calculus and performing phase-plane, phase-space analysis, we are able to categorize different parts of the surface and find the optimal switching policy. The feedback control can then be formed by using this solution. Many numerical examples have been tested and an application to the maneuver of a flexible structure has been demonstrated. The global geometry of the switching functions needs to be investigated for the third- and the fourth-order systems. For practical implementation of this solution for the time-optimal maneuvers, modifications should be considered to accommodate unmodeled factors such as structural damping, higher order modes, and other uncertainties.

Appendix: Brief Review of Strategy of Gulko et al.

The optimal strategy of Gulko et al. from Ref. 7 is briefly summarized here. According to Section 4.5 of Ref. 7, this strategy has been developed for the study of the time-optimal regulator problem in the case of a serially decomposed single-input system, namely,

$$\dot{x}_i = \lambda_i x_i + x_{i+1}, \qquad i = 1, 2, \ldots, n-1 \tag{A1}$$

$$\dot{x}_n = \lambda_n x_n + u/a, \qquad |u| \le 1, \qquad a > 0 \tag{A2}$$

or

$$\dot{x} = Ax + bu \tag{A3}$$

where λ_i are real eigenvalues of the system. A null-controllable initial state (which can be transferred to the state origin in finite time by an admissible control) is given as

$$x(0) = x^\alpha = \left[x_1^\alpha, x_2^\alpha, \ldots, x_n^\alpha\right]^T \tag{A4}$$

Strategy

Consider now that $(n-1)$th-order subsystem formed by deleting the first member of Eq. (A1), the time-optimal subsystem control $u^s(t)$, $0 \le t \le t_{n-1}^s$, which transfers this subsystem from its initial state $x^s(0) = x^{s\alpha} = [x_2^\alpha \quad x_3^\alpha \quad \cdots \quad x_n^\alpha]^T$ to the subspace origin $x^s(t_{n-1}^s) = 0$ in minimum time t_{n-1}^s, will clearly transfer the overall nth-order system from $x(0) = x^\alpha$ to a point on the x_1 state axis, i.e.,

$$x\left(t_{n-1}^s\right) = x^\beta = \left[x_1^\beta \quad 0 \quad \cdots \quad 0\right]^T \tag{A5}$$

The value of the control (at x^α, $t = 0$) for time-optimal control to the origin for the overall nth-order system can now be expressed as

$$u^*(0) = \begin{cases} -\operatorname{sgn}\left(x_1^\beta\right), & x_1^\beta \neq 0 \\ u^s(0), & x_1^\beta = 0 \end{cases} \tag{A6}$$

Remarks

1) The value of x_1^β is usually not available at $t = 0$. But in theory, we assume it can be expressed as a function of the initial state x^α. As stated in Ref. 7, the value of x_1^β is calculated by using a fast model (assume it can be constructed instantaneously) to generate the trajectory from x^α to x^β under u^s; the input to the actual plant is then determined by Eq. (A6). Therefore, this control is classified as predictive control. The optimality of this predictive control strategy has been proven in Ref. 7 and will not be repeated here.

2) Although this strategy has been proven through the serially decomposed system of the form Eqs. (A1) and (A2), it is pointed out in Ref. 7 that the approach can easily be modified to apply to single-input diagonalized systems. This means that the serially decomposed format is not necessary but certainly is convenient for constructing the following control expressions. This also explains the motivation for the linear transformation utilized in the section "Mathematical Model and Transformations," so that the transformed system has a form similar to the serially decomposed format.

3) The extension of this strategy to systems with complex eigenvalues and the application of this strategy to multi-input systems have not been seen in the open literature.

Control Synthesis Problem

As indicated in the preceding remarks, to use this strategy, we need a complete knowledge of the subsystem as expressed in the following two pieces of information.

1) The time-optimal feedback control $u^s(x^s) = -\operatorname{sgn}[s^s(x^s)]$ is explicitly known for the $(n-1)$th-order subsystem, where $s^s(x^s)$ is the switching function of the control for the subsystem.

2) The optimal switching times $t_i^s = T_i^s(x^s)$ for the subsystem state x^s are known explicitly.

Based on this information, the detailed expression for Eq. (A6) can be developed as follows. Starting from an arbitrary null-controllable state $x = [x_1 \; x^{sT}]^T$, at $t = 0$, the end point x^β of the (fictitious) optimal trajectory to the x_1 state axis, i.e., the subspace

origin, is easily characterized (as an explicit function of x) by integrating the full state Eq. (A3) from $t = 0$ to $t = t_{n-1}^s = T_{n-1}^s(x^s)$, i.e.,

$$x^\beta = \exp\left[AT_{n-1}^s(x^s)\right]\left[x - \operatorname{sgn}[s^s(x^s)]\sum_{i=0}^{n-2}(-1)^i \times \int_{T_i^s(x^s)}^{T_{i+1}^s(x^s)} \exp(-A\tau)b\, d\tau\right] \tag{A7}$$

where $T_0^s = 0$. Since e^{At} is in upper triangular form with $\exp(\lambda_i t)$ on the diagonal line, the first element of Eq. (A7) yields

$$\exp\left(\lambda_1 T_{n-1}^s\right)[x_1 + F(x^s)] = x_1^\beta(x)$$

where $F(x^s)$ is a function of the state defined by the subspace only. Since $\exp[\lambda_1 T_{n-1}^s(x^s)] > 0$,

$$\operatorname{sgn}\left[x_1^\beta(x)\right] = \operatorname{sgn}[x_1 + F(x^s)] = \operatorname{sgn}[\xi(x)]$$

and the optimal control Eq. (A6) can be expressed as

$$u^*(x) = -\operatorname{sgn}[s(x)], \qquad s(x) = \begin{cases} \xi(x), & \xi(x) \neq 0 \\ s^s(x^s), & \xi(x) = 0 \end{cases} \tag{A8}$$

Acknowledgments

This research was supported by the U.S. Air Force Office of Scientific Research, Grant F49620-92-J-0165, and NASA, Grant NAGW-2950 (Howard/NASA CSTEA, Center for the Study of Terrestrial and Extraterrestrial Atmospheres).

References

[1]Singh, G., Kabamba, P. T., and McClamroch, N. H., "Planar, Time-Optimal, Rest-to-Rest Slewing Maneuvers of Flexible Spacecraft," *Journal of Guidance, Control, and Dynamics*, Vol. 12, No. 1, 1989, pp. 71–81.

[2]Önsay, T., and Akay, A., "Vibration Reduction of a Flexible Arm by Time-Optimal Open-Loop Control," *Journal of Sound and Vibration*, Vol. 147, No. 2, 1991, pp. 283–300.

[3]Bainum, P. M., and Li, F., "Rapid In-Plane Maneuvering of the Flexible Orbiting SCOLE," *Journal of Astronautical Sciences*, Vol. 39, No. 2, 1991, pp. 233–248.

[4]Hablani, H. B., "Zero-Residual-Energy, Single-Axis Slew of Flexible Spacecraft Using Thrusters: Dynamics Approach," *Journal of Guidance, Control, and Dynamics*, Vol. 15, No. 1, 1992, pp. 104–113.

[5]Liu, Q., and Wie, B., "Robust Time-Optimal Control of Uncertain Flexible Spacecraft," *Journal of Guidance, Control, and Dynamics*, Vol. 15, No. 3, 1992, pp. 597–604.

[6]Barbieri, E., and Özgüner, Ü., "A New Minimum-Time Control Law for a One-Mode Model of a Flexible Slewing Structure," *IEEE Transactions on Automatic Control*, Vol. 38, No. 1, 1993, pp. 142–146.

[7]Ryan, E. P., *Optimal Relay and Saturating Control System Synthesis*, Peter Peregrinus, London, 1982.

[8]Knowles, G., *An Introduction to Applied Optimal Control*, Academic, New York, 1981.

[9]Meirovitch, L., *Dynamics and Control of Structures*, Wiley, New York, 1990.

[10]Hall, H. S., and Knight, S. R., *Higher Algebra*, MacMillan, London, 1957.